Research Article

Manisha, Nidhi, Anuj Kumar*

Assessing the impact of information-induced self-protection on Zika transmission: A mathematical modeling approach

https://doi.org/10.1515/cmb-2023-0123
received October 18, 2023; accepted January 28, 2024

Abstract: As per the World Health Organization's (WHO's) suggestions, personal protection via adopting precautionary measures is one of the most effective control aspects to avoid Zika infection in the absence of suitable medical treatment. This personal protection further can be enhanced and explored by propagating information about disease prevalence. Therefore, in this study, we wish to see the effect of information on Zika transmission by formulating a compartmental mathematical model that quantifies the effect of an individual's behavioral response as self-protection due to information. Furthermore, the basic reproduction number was calculated using the next-generation matrix technique. The model analysis was carried out to determine the local and global stability properties of equilibrium points. In addition, the model shows the occurrence of forward bifurcation when the reproduction number crosses unity. To understand the impact of various model parameters, we conducted a sensitivity analysis using both the normalized sensitivity index and the partial rank correlation coefficient methods. Moreover, we performed numerical simulations to assess the influence of important parameters on the model's behavior for Zika prevalence. Our study accentuates that as information-induced self-protection increases, the prevalence of Zika infection will be at a very minimum level, and this observation is in line with WHO suggestions.

Keywords: compartmental model, information-induced self-protection, reproduction number, bifurcation, global stability

MSC 2020: 34D20, 92B05, 92D30

1 Introduction

Vector-borne diseases transmitted by carriers such as mosquitoes, flies, and ticks pose a significant health risk and have far-reaching economic repercussions globally. Mosquitoes are of particular concern as they are vectors for a range of serious illnesses that greatly impact public health. Therefore, mosquito-borne diseases such as malaria, Zika, dengue, and Chikungunya remain a major global issue. The World Health Organization (WHO) data indicate that dengue alone has an annual global incidence in the millions, causing widespread illness and fatalities [14,38]. Moreover, vector-borne diseases annually affect approximately two million people, resulting in huge mortality and morbidity [10]. These diseases also have considerable economic, public health, and social ramifications. Since the last few years, the outbreak of the Zika virus has been an additional

*** Corresponding author: Anuj Kumar**, School of Mathematics, Thapar Institute of Engineering & Technology, Patiala 147004, India, e-mail: anujdubey17@gmail.com
Manisha: School of Mathematics, Thapar Institute of Engineering & Technology, Patiala 147004, India, e-mail: manishamalik2000@gmail.com
Nidhi: School of Mathematics, Thapar Institute of Engineering & Technology, Patiala 147004, India, e-mail: nidhisingla31000@gmail.com

source of concern for public health, and 89 countries have documented the evidence of Zika prevalence till December 2021 [39]. Therefore, among all vector-borne diseases, the control of Zika transmission is one of the most challenging scenarios, as it causes a large number of deaths and illnesses. Therefore, understanding the dynamics of mosquito-borne diseases, especially Zika, is essential for developing precise and effective control measures. Researchers and academicians from various fields worldwide have shown considerable interest in studying the dynamics of vector-borne diseases [12,30,36,37].

The intricate nature of Zika transmission necessitates a comprehensive understanding of its dynamics and the identification of effective strategies to mitigate them. While it presents a significant challenge for governments and policymakers to curb the spread of infection, several approaches and methodologies are employed. One such approach is mathematical modeling, which plays a crucial role in providing a detailed understanding of disease dynamics through the illustration of interactions between vectors (such as mosquitoes) and human populations. Furthermore, mathematical models offer insights that guide the formulation of targeted control measures to reduce infection risk. As a result, numerous mathematical models have been developed for Zika and other vector-borne diseases. These models aim to predict disease patterns and establish various control strategies to minimize or eliminate the risk of infection [1,15,19,21,26,32,36,37]. Thus, before formulating a model, it is important to know the biology and interaction of vectors such as Zika, dengue, and malaria that cause the outbreaks of diseases. Numerous factors are causing outbreaks of the aforesaid diseases. For instance, the occurrence of the Zika virus is affected by a variety of conditions, including seasonal changes, climatic circumstances, demography, migration of population, etc. Zika transmits through the bite of *Aedes aegypti* mosquitoes, whereas it also transmits through vertical transmission, such as sexual contact, from the mother to her fetus during pregnancy, and blood transfusions. After a few days (3–14 days), the infected person shows some symptoms such as muscle pain, redness of the eyes, mild fever, and headache [40]. These symptoms give directions for early detection and treatment. If prevention is not provided in time, then such diseases will result in high mortality. Based on the aforesaid observations, many mathematical models have been formulated and studied.

For instance, Ndaïrou et al. analyzed a Zika model on the women population in which they divided the entire women population and female mosquito population into different compartments [29]. They investigated that it is essential to implement control measures that reduce the average number of daily bites and the transmission probability from infected mosquitoes to susceptible pregnant women to reduce the number of new infections. Biswas et al. proposed and analyzed a deterministic Zika virus model in which they quantified the vertical transmission through sexual contact along with the effects of human awareness and vector control [3]. The authors also studied the effect of sexual transmission on the basic reproduction number and epidemic growth rate and investigated whether the dominance of the Zika virus could be suppressed by lowering the sexual transmission rate. Recently, Maqrashi et al. discussed a compartmental model for the Zika virus by considering direct and indirect transmission along with vertical transmission [2]. They simulated and fitted their proposed model with the data of Brazil and Colombia, estimated the reproduction number R_0, and found that if R_0 is less than one, then the disease will die out (for both countries). In 2023, to explore the effect of sexual transmission on women and microcephaly cases, Ibrahim and Dénes analyzed and fitted a compartmental Zika model for Colombia between 2015 and 2017 [16]. Their sensitivity analysis concluded that preventing mosquito bites and providing protection during sexual contact are the most effective ways to reduce Zika prevalence.

On the Zika outbreak and control, WHO suggests that individuals' personal protection by taking suitable protective measures, such as bed nets, mosquito repellent, and full-body clothing, is one of the crucial interventions to avoid infection [40]. Moreover, we also know that whenever an outbreak happens, the information about it also spreads through electronic and social media, newspapers, television and personal interactions. This information influences individuals' behaviors, leading them to adopt precautionary measures to reduce the infection. Consequently, information-induced behavioral change has emerged as a significant factor (suggested by WHO) among various control measures. Therefore, in this study, our main objective is to explore the impact of information on Zika transmission. Numerous researchers have investigated the impact of information-induced behavioral change on disease dynamics [17,20,25,32]. For instance, Kassa and Ouhinou formulated a mathematical model that incorporates behavioral change and treatment. Their model divided

the human population into four compartments: susceptible, educated (those who take self-protective measures due to disease awareness), infected, and treated. They demonstrated that behavioral change as an intervention is more effective than treatment alone [18]. Kumar et al. introduced a nonlinear susceptible infected recovered susceptible compartmental model to quantify the effect of information on an individual's behavioral response during an epidemic [20]. They found that combining both behavioral responses due to information and saturated treatment as control measures effectively reduces the risk of infection. De Lara-Tuprio et al. also assessed the impact of awareness on susceptible humans by proposing a compartmental model for dengue transmission with time lags in the incubation periods of humans and mosquitoes [8]. They discovered that higher awareness levels, characterized by the adoption of protective measures, significantly contribute to reducing the dengue virus. Recently, Kumar and Srivastav explored the importance of self-protection due to information in a nonlinear susceptible exposed infected recovered model [19]. Their findings emphasized the role of screening in preventing future infections (exposed individuals) at a lower cost compared to treating the infected population.

As per the above discussion, nonpharmaceutical controls (e.g., use of bed nets, mosquito repellent, and use of insecticides) along with some medical treatments are crucial in reducing the infection risk. Moreover, the widespread occurrence of vector-borne diseases has led to considerable social and economic challenges, putting a heavy disease burden on countries globally. As a result, it is essential to study how these control measures influence disease spread. Many authors have proposed mathematical models that quantify mainly pharmaceutical control measures (prevention) that reduce the infection count but increase the economic load. The effect of self-protection due to information (self-protection) is found to be one of the useful controls (nonpharmaceutical). Therefore, in this study, we formulate a model that quantifies the effect of information-based self-protection as a control intervention. To fulfill the said purpose, we consider a basic mathematical model (SEI type) for a vector-transmitted disease proposed by Brauer et al. [4], and the model is given by

$$\left.\begin{aligned}
\frac{\mathrm{d}S}{\mathrm{d}t} &= -\frac{\beta S I_v}{N_v} - \frac{\alpha S I}{N} \\
\frac{\mathrm{d}E}{\mathrm{d}t} &= \frac{\beta S I_v}{N_v} + \frac{\alpha S I}{N} - \kappa E \\
\frac{\mathrm{d}I}{\mathrm{d}t} &= \kappa E - \gamma I \\
\frac{\mathrm{d}S_v}{\mathrm{d}t} &= \mu N_v - \mu S_v - \frac{\beta_v S_v I}{N} \\
\frac{\mathrm{d}E_v}{\mathrm{d}t} &= \frac{\beta_v S_v I}{N} - (\mu + \eta) E_v \\
\frac{\mathrm{d}I_v}{\mathrm{d}t} &= \eta E_v - \mu I_v
\end{aligned}\right\} \tag{1}$$

The rest of the manuscript is classified in the following order: in the consecutive section, a mathematical model is proposed; in Section 3, the analysis of the model is performed, followed by bifurcation analysis around $R_0 = 1$ in Section 4; Section 5 involves performing local and global sensitivity analysis; Section 6 explores the impact of various parameters through numerical simulations; and finally, in Section 7, our findings are concluded.

2 Formulation of mathematical model

In this section, we develop a compartmental mathematical model for Zika virus in which the entire human population (N) is categorized into three subgroups: susceptible individuals (S), exposed individuals (E), and infected individuals (I). Similarly, the total vector population (N_v) is split into three sections: susceptible vectors (S_v), exposed vectors (E_v), and infected vectors (I_v). Exposed individuals are those who have contracted the infection but are not capable of spreading it, whereas infected individuals can both carry and transmit the infection. It is important to note that the Zika virus can spread not only through mosquitoes but also via direct

interactions such as sexual intercourse, mother-to-child transmission, and blood transfusions. Consequently, it becomes vital to calculate the impact of direct transmission on the infection spread. To achieve this, a term $\frac{\alpha SI}{N}$ was introduced into the susceptible human population, representing direct transmission, in model (1), as given by Brauer et al. [4]. The parameter α denotes the rate at which susceptible humans directly transition to the infected human compartment. Moreover, prevention of the Zika virus can be achieved through self-protective measures, which include practices like safe sexual contact, applying mosquito repellents, wearing full-body clothes, covering water storage containers, use of insecticides, etc. Awareness of these preventive measures spreads rapidly through various media channels, such as newspapers and television, prompting the susceptible population to adopt these measures and transition to the recovered class. Therefore, we introduce the term θS in the susceptible population to represent information-induced self-protection where the parameter θ indicates the rate at which the susceptible population moves directly to the recovered class as a result of self-protection [20]. Another important feature is the demographic impact on population which has not been considered in model (1) by Brauer et al. [4]. As it has important biological meaning in vector-borne diseases, we further quantify the demographic effects in our model formulation. Considering all the aforementioned modifications and factors, the mathematical model is structured as follows:

$$\left.\begin{aligned}
\frac{\mathrm{d}S}{\mathrm{d}t} &= \mu_1 N - \frac{\beta S I_v}{N_v} - \frac{\alpha S I}{N} - \mu_1 S - \theta S \\
\frac{\mathrm{d}E}{\mathrm{d}t} &= \frac{\beta S I_v}{N_v} + \frac{\alpha S I}{N} - \kappa E - \mu_1 E \\
\frac{\mathrm{d}I}{\mathrm{d}t} &= \kappa E - \gamma I - \mu_1 I \\
\frac{\mathrm{d}S_v}{\mathrm{d}t} &= \mu N_v - \mu S_v - \frac{\beta_v S_v I}{N} \\
\frac{\mathrm{d}E_v}{\mathrm{d}t} &= \frac{\beta_v S_v I}{N} - (\mu + \eta) E_v \\
\frac{\mathrm{d}I_v}{\mathrm{d}t} &= \eta E_v - \mu I_v
\end{aligned}\right\}, \tag{2}$$

with an initial human population of $S(0) > 0$, $E(0) \geq 0$, and $I(0) \geq 0$, and an initial vector population of $S_v(0) > 0$, $E_v(0) \geq 0$, and $I_v(0) \geq 0$, all model parameters are assumed to be nonnegative. The recruitment rates for the human and vector populations are represented by $\mu_1 N$ and μN_v, respectively. The parameter β denotes the disease transmission rate that occurs when a susceptible individual encounters an infected mosquito, causing the individual to transition to the exposed class. After a certain duration, the exposed human shifts to the infected class at a rate κ. The infected population undergoes recovery at a rate γ. The interaction rate between infected humans and susceptible vectors is indicated by β_v. The exposed vectors progress to the infected class at a rate η. In addition, μ_1 and μ represent the natural death rates of human and vector populations, respectively.

2.1 Positivity and boundedness of the solutions

This section shows the model's biological relevance by establishing the positivity and boundedness of system variables.

Theorem 1. *The solution of model system* (2) *in* $\mathbb{R}^6_+$ *remains positive for all time.*

Proof. From model system (2), the rate equations are given as: $\frac{\mathrm{d}S}{\mathrm{d}t}\Big|_{S=0} = \mu_1 N > 0$, $\frac{\mathrm{d}E}{\mathrm{d}t}\Big|_{E=0} = \frac{\beta S I_v}{N_v} + \frac{\alpha S I}{N} > 0$, $\frac{\mathrm{d}I}{\mathrm{d}t}\Big|_{I=0} = \kappa E > 0$, $\frac{\mathrm{d}S_v}{\mathrm{d}t}\Big|_{S_v=0} = \mu N_v > 0$, $\frac{\mathrm{d}E_v}{\mathrm{d}t}\Big|_{E_v=0} = \frac{\beta_v S_v I}{N} > 0$, $\frac{\mathrm{d}I_v}{\mathrm{d}t}\Big|_{I_v=0} = \eta E_v > 0$.

Note from above equation that nonnegativity of all rates are ensured on bounding planes of the nonnegative cone of $\mathbb{R}^6$. This infers that if we start in the interior of this cone, then we shall always remain in this cone due to the inward direction of the vector field on all the bounding planes. Hence, positive solutions for the system (2) are ensured. □

Theorem 2. *The solution of model system* (2) *in* $\mathbb{R}^6_+$ *remains bounded for all time.*

Proof. From system (2), we have that the human population is $N(t) = S(t) + E(t) + I(t)$. Furthermore,

$$\frac{\mathrm{d}N}{\mathrm{d}t} = \frac{\mathrm{d}S}{\mathrm{d}t} + \frac{\mathrm{d}E}{\mathrm{d}t} + \frac{\mathrm{d}I}{\mathrm{d}t} = \mu_1 N - \mu_1 S - \theta S u_1 - \mu_1 E - \gamma I - \mu_1 I = -\theta S - \gamma I \leq 0.$$

Thus, $\sup_{t\to\infty} N \leq C_0$. Therefore, all solutions S, E, and I are bounded by a constant C_0. Similarly, the vector population is $N_v(t) = S_v(t) + E_v(t) + I_v(t)$, which gives

$$\frac{\mathrm{d}N_v}{\mathrm{d}t} = 0 \Rightarrow N_v(t) = C_1$$

Thus, $\sup_{t\to\infty} N_v \leq C_1$. Hence, all solutions S_v and $E_v I_v$ are bounded by a constant C_1. □

Thus, using the above positivity and boundedness, the biologically feasible region of the model system (2) is the following invariant set:

$$\Gamma = \{(S, E, I, S_v, E_v, I_v) \in \mathbb{R}^6_+ | 0 \leq N(t) \leq C_0, 0 \leq N_v(t) \leq C_1\}.$$

3 Equilibrium analysis

3.1 Disease-free equilibrium (DFE) E_0

The DFE of the model system (2) is given below:

$$E_0 = \left(S_0, 0, 0, S_{v_0}, 0, 0\right) = \left(\frac{\mu_1 N}{\mu_1 + \theta}, 0, 0, N_v, 0, 0\right).$$

3.2 The basic reproduction number (R_0)

The basic reproduction number (R_0) is defined as the number of secondary infection caused by a single infected individual in an entire infective period [34]. To compute the reproduction number, we followed the next generation matrix method discussed in [34]. Consider $x \equiv (E, I, E_v, I_v)$, then we have

$$\frac{\mathrm{d}x}{\mathrm{d}t} = \Im(x) - \nu(x),$$

where $\Im(x) = \begin{pmatrix} \frac{\beta S I_v}{N_v} + \frac{\alpha S I}{N} \\ 0 \\ \frac{\beta_v S_v I}{N} \\ 0 \end{pmatrix}$, $\nu(x) = \begin{pmatrix} (\kappa + \mu_1)E \\ -\kappa E + (\gamma + \mu_1)I \\ (\mu + \eta)E_v \\ -\eta E_v + \mu I_v \end{pmatrix}$. The Jacobian matrix of $\Im(x)$ and $\nu(x)$ at DFE E_0 are:

$$F = (D\mathfrak{I}(x))_{E_0} = \begin{pmatrix} 0 & \frac{\alpha SI}{N} & 0 & \frac{\beta S}{N_v} \\ 0 & 0 & 0 & 0 \\ 0 & \frac{\beta_v S_v}{N} & 0 & 0 \\ 0 & 0 & 0 & 0 \end{pmatrix}, \quad V = (Dv(x))_{E_0} = \begin{pmatrix} \kappa + \mu_1 & 0 & 0 & 0 \\ -\kappa & \gamma + \mu_1 & 0 & 0 \\ 0 & 0 & \mu + \eta & 0 \\ 0 & 0 & -\eta & \mu \end{pmatrix}.$$

From above, we have

$$FV^{-1} = \begin{pmatrix} \frac{\alpha S\kappa}{N(\kappa + \mu_1)(\gamma + \mu_1)} & \frac{\alpha S}{N(\gamma + \mu_1)} & \frac{\beta^* S^* \eta}{N_v(\mu + \eta)\mu} & \frac{\beta^* S}{N_v{}^*\mu} \\ 0 & 0 & 0 & 0 \\ \frac{\beta_v S_v \kappa}{(\kappa + \mu_1)(\gamma + \mu_1)} & \frac{\beta_v S_v}{(\gamma + \mu_1)} & 0 & 0 \\ 0 & 0 & 0 & 0 \end{pmatrix}.$$

The largest eigenvalue of the matrix FV^{-1} is defined as the reproduction (R_0) of the model system (2) and is given as follows:

$$R_0 = R_{01} + \sqrt{R_{02} + R_{01}^2},$$

where $R_{01} = \frac{\alpha\kappa S_0}{2aNb}$ and $R_{02} = \frac{\eta\kappa\beta\beta_v S_0 S_{v0}}{ac\mu NN_v b}$, $a = \kappa + \mu_1$, $b = \gamma + \mu_1$, $c = \mu + \eta$, $e = \mu_1 + \theta$.

3.3 Endemic equilibrium point (E_1)

Considering a, b, c, $d = \mu$, e and putting right-hand side of the system (2) equal to zero, we have

$$\begin{aligned} -\frac{\beta SI_v}{N_v} - \frac{\alpha SI}{N} + \mu_1 N - eS &= 0 \\ \frac{\beta SI_v}{N_v} + \frac{\alpha SI}{N} - aE &= 0 \\ \kappa E - bI &= 0 \\ \mu N_v - dS_v - \frac{\beta_v S_v I}{N} &= 0 \\ \frac{\beta_v S_v I}{N} - cE_v &= 0 \\ \eta E_v - dI_v &= 0. \end{aligned} \tag{3}$$

Solving the above system of equations, we have an endemic equilibrium point $E_1 = (S^*, E^*, I^*, S_v^*, E_v^*, I_v^*)$, whose components are $S^* = \frac{\mu_1 N}{\frac{\beta S^* I_v^*}{N_v} + \frac{\alpha S^* I^*}{N} + e}$, $E^* = \frac{1}{a}\left(\frac{\beta S^* I_v^*}{N_v} + \frac{\alpha S^* I^*}{N}\right)$, $S_v^* = \frac{\mu N_v}{d + \frac{\beta_v I^*}{N}}$, $E_v^* = \frac{\beta_v S_v^*}{cN}$, $I_v^* = \frac{\eta E_v^*}{\mu}$, and I^* is positive root of equation given as follows:

$$f(I) = B_{11}I^2 + B_{12}I + B_{13} = 0, \tag{4}$$

where $B_{11} = abcda\beta_v$, $B_{12} = abcd^2N\alpha + acd^2Nu_2\alpha + abcd^2ea_1N + abcde\beta_v\mu + ab\eta\mu\beta\beta_v N - cdN\alpha\beta_v\kappa\mu_1$, and $B_{13} = abcd^2eN^2((1 - R_0)(1 + R_0 - 2R_{01}))$. Note that B_{11} is always positive, and other coefficients may change their sign. Clearly, if $R_0 > 1$ ($B_{13} < 0$ and positivity of $(1 + R_0 - 2R_{01})$ is given in Section 3.4), then the equation (4) has unique positive root; hence, $I^* = \frac{-B_{12} + \sqrt{B_{12}^2 - 4B_{11}B_{13}}}{2B_{11}}$; hence, the model system (2) has an unique endemic equilibrium point E_1.

Theorem 3. *The model system* (2) *has*

(i) *a DFE* $E_0 = \left(\frac{\mu_1 N}{\mu_1+\theta}, 0, 0, N_v, 0, 0\right)$, *which always exist.*

(ii) *the unique endemic equilibrium* $E_1 = (S^*, E^*, I^*, S_v^*, E_v^*, I_v^*)$, *which exist whenever* $R_0 > 1$.

Remark 1. The system may have multiple endemic equilibrium which depends on the sign of coefficients of the equation (4).

3.4 Local analysis of equilibrium points E_0 and E_1

The local stability of equilibrium points is established for the model system (2) using the Jacobian matrix, which is defined as follows:

$$J = \begin{pmatrix} -e - \frac{\alpha I}{N} - \frac{\beta I_v}{N_v} & 0 & \frac{-\alpha S}{N} & 0 & 0 & \frac{-\beta S}{N_v} \\ \frac{\alpha I}{N} + \frac{\beta I_v}{N_v} & -a & \frac{\alpha S}{N} & 0 & 0 & \frac{\beta S}{N_v} \\ 0 & \kappa & -b & 0 & 0 & 0 \\ 0 & 0 & \frac{\beta_v S_v}{N} & -d - \frac{\beta_v I}{N} & 0 & 0 \\ 0 & 0 & \frac{\beta_v S_v}{N} & \frac{\beta_v I}{N} & -c & 0 \\ 0 & 0 & 0 & 0 & \eta & -d \end{pmatrix}.$$

The Jacobian matrix at E_0 is given by

$$J|_{E_0} = \begin{pmatrix} -e & 0 & -\frac{\alpha S_0}{N} & 0 & 0 & -\frac{\beta S_0}{N_v} \\ 0 & -a & \frac{\alpha S_0}{N} & 0 & 0 & \frac{\beta S_0}{N_v} \\ 0 & \kappa & -b & 0 & 0 & 0 \\ 0 & 0 & -\frac{\beta_v S_{v0}}{N} & -d & 0 & 0 \\ 0 & 0 & \frac{\beta_v S_{v0}}{N} & 0 & -c & 0 \\ 0 & 0 & 0 & 0 & \eta & -d \end{pmatrix}. \tag{5}$$

Clearly, the two eigenvalues $l_1 = -e$, $l_2 = -d$ are always negative, and other eigenvalues are given by the following characteristic equation:

$$l^4 + A_1 l^3 + A_2 l^2 + A_3 l + A_4 = 0, \tag{6}$$

where $A_1 = a + b + c + d$, $A_2 = bd + ab + ad + cb + cd + ac - \frac{\alpha\kappa S}{N}$, $A_3 = abd + cbd + abc + acd - \frac{\alpha\kappa Sc}{N} - \frac{\alpha\kappa Sd}{N}$, and $A_4 = acdb(1 - R_0)(R_0 + 1 - 2R_{01})$. Note that A_1 is always positive and A_4 is positive when $R_0 < 1$ as $R_0 + 1 - 2R_{01}$ is always positive. Here, the positivity as follows: Now putting the value of R_0 in the aforesaid expression, we obtain $R_{01} + 1 + \sqrt{R_{01}^2 + R_{02}} - 2R_{01} = 1 + \sqrt{R_{01}^2 + R_{02}} - R_{01}$. Clearly, one can see that $\sqrt{R_{01}^2 + R_{02}}$ is always greater than equal to R_{01}, as R_{01} and R_{02} are always positive. Hence, by using Routh-Hurwitz criterion, it is ensured that E_0 is locally asymptotically stable if the conditions $A_1 > 0$, $A_4 > 0$, $A_1A_2 - A_3 > 0$, and $(A_1A_2 - A_3)A_3 - A_1^2A_4 > 0$ hold true, and the corresponding result is stated below.

Theorem 4. *The DFE* (E_0) *of system* (2) *is locally asymptotically stable if* $A_1 > 0$, $A_4 > 0$, $A_1A_2 - A_3 > 0$, *and* $(A_1A_2 - A_3)A_3 - A_1^2A_4 > 0$ *when* $R_0 < 1$.

The Jacobian matrix at endemic equilibrium point E_1 is given as follows:

$$J|_{E_1} = \begin{pmatrix} -e - \frac{\alpha I^*}{N} - \frac{\beta I_v^*}{N_v} & 0 & \frac{-\alpha S^*}{N} & 0 & 0 & -\frac{\beta S^*}{N_v} \\ \frac{\alpha I^*}{N} + \frac{\beta I_v^*}{N_v} & -a & \frac{\alpha S^*}{N} & 0 & 0 & \frac{\beta S^*}{N_v} \\ 0 & \kappa & -b & 0 & 0 & 0 \\ 0 & 0 & -\frac{\beta_v S_v^*}{N} & -d - \frac{\beta_v I^*}{N} & 0 & 0 \\ 0 & 0 & \frac{\beta_v S_v^*}{N} & \frac{\beta_v I^*}{N} & -c & 0 \\ 0 & 0 & 0 & 0 & \eta & -d \end{pmatrix}.$$

Assume $a_1 = -e - \frac{\alpha I^*}{N} - \frac{\beta I_v^*}{N_v}$, $a_2 = \frac{\alpha I^*}{N} + \frac{\beta I_v^*}{N_v}$, $a_3 = -b - \frac{u_2}{(1+\alpha I^*)^2}$, $a_4 = -d - \frac{\beta_v I^*}{N}$, $a_5 = \frac{-\alpha S^*}{N}$, $a_6 = \frac{\beta S^*}{N_v}$, $a_7 = \frac{\beta_v S_v^*}{N}$, and $a_8 = \frac{\beta_v I^*}{N}$. Then, the characteristic polynomial of $J|_{E_1}$ is given as follows:

$$l^6 + P_{11}l^5 + P_{12}l^4 + P_{13}l^3 + P_{14}l^2 + P_{15}l + P_{16} = 0, \tag{7}$$

where $P_{11} = a - a_1 - a_3 - a_4 + c + d$, $P_{12} = -aa_1 - aa_3 + a_1a_3 - aa_4 + a_1a_4 + a3a4 + ac - a1c - a3c - a_4c + ad - a_1d - a_3d - a_4d + cd - a_5\kappa$, $P_{13} = aa_1a_3 + aa_1a_4 + aa_3a_4 - a_1a_3a_4 - aa_1c - aa_3c + a_1a_3c - aa_4c + a_1a_4c + a_3a_4c - aa_1d - aa_3d + a_1a_3d - aa_4d + a_1a_4d + a_3a_4d + acd - a_1cd - a_3cd - a_4cd + a_1a_5\kappa + a_2a_5\kappa + a_4a_5\kappa - a5c\kappa - a_5\mathrm{d}\kappa$, $P_{14} = -a_1a_3a_4c - a_1a_3a_4d + a_1a_3cd + a_1a_4cd + a_3a_4cd + a(-a_1a_3a_4 + a_1a_3c + a_1a_4c + a_3a_4c + (a_1a_3 + a_1a_4 + a_3a_4 - (a_1 + a_3 + a_4)c)d) + a_5(-a_2a_4 + a_2c + a_4c + (a_2 + a_4 - c)d + a_1(-a_4 + c + d))\kappa - a_6a_7\eta\kappa$, $P_{15} = aa_3a_4cd - a_1a_3a_4cd + aa_1(a_3cd + a_4cd - a_3a_4(c + d)) + a_5(a_2cd + a_4cd - a_2a_4(c + d))\kappa + a_6a_7(a_2 + a_4 + a_8)\eta\kappa + a_1(a_5cd - a_4a_5(c + d) + a_6a_7\eta)\kappa$, $P_{16} = -aa_1a_3a_4cd + a_1a_4a_5c\mathrm{d}\kappa - a_2a_4\ a_5c\mathrm{d}\kappa - a_1a_4a_6a_7\eta\kappa - a_2a_4\ a_6a_7\eta\kappa - a_1a_6a_7a_8\eta\kappa - a_2a_6a_7a_8\eta\kappa$. Let us consider: $C_1 = P_{11}$, $C_2 = \begin{pmatrix} P_{11} & 1 \\ P_{13} & P_{12} \end{pmatrix}$, $C_3 = \begin{pmatrix} P_{11} & 1 & 0 \\ P_{13} & P_{12} & P_{11} \\ P_{15} & P_{14} & P_{13} \end{pmatrix}$, $C_4 = \begin{pmatrix} P_{11} & 1 & 0 & 0 \\ P_{13} & P_{12} & P_{11} & 1 \\ P_{15} & P_{14} & P_{13} & P_{12} \\ 0 & P_{16} & P_{15} & P_{14} \end{pmatrix}$,

$C_5 = \begin{pmatrix} P_{11} & 1 & 0 & 0 & 0 \\ P_{13} & P_{12} & P_{11} & 1 & 0 \\ P_{15} & P_{14} & P_{13} & P_{12} & P_{11} \\ 0 & P_{16} & P_{15} & P_{14} & P_{13} \\ 0 & 0 & 0 & P_{16} & P_{15} \end{pmatrix}$, $C_6 = P_{16}$.

Clearly, Routh-Hurwitz criteria infers that E_1 is locally asymptotically stable if $\det(C_i) > 0$, $i = 1 - 6$, and the corresponding result is given below.

Theorem 5. *The endemic equilibrium point* E_1 *is locally asymptotically stable if* $\det(C_i) > 0, i = 1 - 6$, *and* $R_0 > 1$.

3.5 Global stability of DFE

To establish the global stability of the DFE, we follow the method discussed in Castillo-Chavez et al. [5]. Consider if system (2) can be written in the following form:

$$\begin{aligned} \frac{\mathrm{d}X}{\mathrm{d}t} &= F(X, Y), \\ \frac{\mathrm{d}Y}{\mathrm{d}t} &= G(X, Y) \quad \text{with } G(X, 0) = 0, \end{aligned} \tag{8}$$

where $X \in \mathbb{R}^{n_1}$ denotes the uninfected population compartments and $Y \in \mathbb{R}^{n_2}$ denotes the infected population compartments, then n_1 and n_2 are positive integers. Let $U_0 = (X_0, 0)$ be the DFE of system (3). Consider the following two assumptions:

(H1) For $\frac{\mathrm{d}X}{\mathrm{d}t} = F(X, 0)$, X_0 is globally asymptotically stable.

(H2) $G(X, Y) = AY - \hat{G}(X, Y)$ and $\hat{G}(X, Y) \geq 0$ for $(X, Y) \in \Omega$, where $A = D_Y G(X_0, 0)$ is an M-matrix and Ω is the biologically feasible region.

Theorem 6. *The DFE $U_0 = (X_0, 0)$ of equation* (8) *is globally asymptotically stable for $R_0 < 1$, provided the assumptions (H_1) and (H_2) are satisfied.*

To show the global stability of DFE E_0, we consider the model system (2) in the following form:

$$F(X, Y) = \left(\mu_1 N - \frac{\beta S I_v}{N_v} - \frac{\alpha S I}{N} - \mu_1 S - \theta S, \mu N_v - \mu S_v - \frac{\beta_v S_v I}{N} \right) \tag{9}$$

$$G(X, Y) = \left(\frac{\beta S I_v}{N_v} + \frac{\alpha S I}{N} - \kappa E - \mu_1 E, \kappa E - \gamma I - \mu_1 I, \frac{\beta_v S_v I}{N} - (\mu + \eta) E_v, \eta E_v - \mu I_v \right)^T, \tag{10}$$

with $G(X, 0) = 0$, where $X = (S, S_v)$ and $Y = (E, I, E_v, I_v)^T$. The DFE of system (2) is $U_0 = E_1 = (X_0, 0)$ with $X_0 = \left(\frac{\mu_1 N}{\mu_1 + \theta}, N_v \right)$. Clearly, X_0 is globally asymptotically stable for $\frac{\mathrm{d}X}{\mathrm{d}t} = F(X, 0)$ as $X \to \left(\frac{\mu_1 N}{\mu_1 + \theta}, N_v \right)$ when $t \to \infty$. Furthermore,

$$G(X, Y) = \begin{pmatrix} a - \kappa - \mu_1 & \frac{\alpha S_0}{N} & 0 & d\frac{\beta S_0}{N_v} \\ \kappa & -\gamma\mu_1 & 0 & 0 \\ 0 & \frac{\beta_v S_{v_0}}{N} & -\mu - \eta & 0 \\ 0 & 0 & \eta & -\mu \end{pmatrix} \begin{pmatrix} E \\ I \\ E_v \\ I_v \end{pmatrix} - \begin{pmatrix} \left(\frac{\alpha I}{N} + \frac{\beta I_v}{N_v} \right)(S_0 - S) \\ 0 \\ \frac{\beta_v I}{N}(S_{v_0} - S_v) \\ 0 \end{pmatrix}.$$

Consider

$$A = \begin{pmatrix} a - \kappa - \mu_1 & \frac{\alpha S_0}{N} & 0 & d\frac{\beta S_0}{N_v} \\ \kappa & -\gamma\mu_1 & 0 & 0 \\ 0 & \frac{\beta_v S_{v_0}}{N} & -\mu - \eta & 0 \\ 0 & 0 & \eta & -\mu \end{pmatrix} \quad \text{and} \quad \hat{G}(X, Y) = \begin{pmatrix} \left(\frac{\alpha I}{N} + \frac{\beta I_v}{N_v} \right)(S_0 - S) \\ 0 \\ \frac{\beta_v I}{N}(S_{v_0} - S_v) \\ 0 \end{pmatrix}.$$

Note that, $S \leq S_0$ and $S_v \leq S_{v_0}$ which gives that $\hat{G}(X, Y) \geq 0$. Furthermore, A is M-matrix in Ω. Hence, we can say that assumptions (H_1) and (H_2) are true. We summarize the above discussion in the following:

Theorem 7. *The DFE E_0 of system* (2) *is globally asymptotically stable for $R_0 < 1$.*

3.6 Global stability of endemic equilibrium E_1

In this part of the manuscript, the global stability property of the endemic equilibrium point is measured with the help of geometric approach method given by Li and Muldowney [24]. For this purpose, we first establish the uniform persistence of the model system (2).

Lemma 1. *The model system* (2) *is uniformly persistent, i.e., there exists a positive constant* **C** *such that*

$$\liminf_{t\to\infty}\{S(t), E(t), I(t), S_v(t), E_v(t), I_v(t)\} \geq \mathbf{C}.$$

Proof. We know that Theorem 4 ensures the instability of the DFE E_0 when $R_0 > 1$. Hence, the instability of the DFE leads the uniform persistence of the system when $R_0 > 1$ using the uniform persistence result [11, 22,24]. Thus, the uniform persistence of model system (2) is guaranteed. □

Now, we establish the global stability property of the unique endemic equilibrium E_1 using the geometric approach [24] (as discussed in Appendix A). For this purpose, we consider a subsystem of the proposed model system (2) as follows:

$$\begin{aligned}\frac{\mathrm{d}I}{\mathrm{d}t} &= \kappa E - \gamma I - \mu_1 I,\\ \frac{\mathrm{d}I_v}{\mathrm{d}t} &= \eta E_v - \mu I_v.\end{aligned} \tag{11}$$

The corresponding Jacobian matrix to the subsystem (11) is given as follows:

$$J_1 = \begin{pmatrix} -\gamma & 0 \\ 0 & -\mu \end{pmatrix}.$$

Now, we compute the corresponding second additive compound matrix [23,28], which is given as follows:

$$J_1^{[2]} = -(\mu + \gamma).$$

Further, we define the following function:

$$Q = Q(I, I_v) \equiv \mathrm{diag}\left(\frac{I}{I_v}, \frac{I}{I_v}\right),$$

and the corresponding two matrices are $Q^{-1} = \mathrm{diag}\left(\frac{I_v}{I}, \frac{I_v}{I}\right)$ and $Q_f = \mathrm{diag}\left(\frac{\dot{I}}{I_v} - \frac{I\dot{I}_v}{I_v^2}, \frac{\dot{I}}{I_v} - \frac{I\dot{I}_v}{I_v^2}\right)$. Now, we also determine $Q_f Q^{-1} = \mathrm{diag}\left(\frac{\dot{I}}{I_v} - \frac{\dot{I}_v}{I_v}, \frac{\dot{I}}{I_v} - \frac{\dot{I}_v}{I_v}\right)$ and $QJ_1^{[2]}Q^{-1} = \mathrm{diag}(-(\mu + \gamma), -(\mu + \gamma))$.

Furthermore, the required matrix $\mathbb{B}$ is defined as follows:

$$\mathbb{B} = \begin{pmatrix} B_{11} & B_{12} \\ B_{21} & B_{22} \end{pmatrix},$$

where $B_{11} = -(\mu + \gamma) + \frac{\dot{I}}{I_v} - \frac{\dot{I}_v}{I_v}$, $B_{12} = 0$, $B_{21} = 0$, and $B_{22} = -(\mu + \gamma) + \frac{\dot{I}}{I_v} - \frac{\dot{I}_v}{I_v}$.

The Lozinskiĭ measure is defined as follows:

$$\Upsilon(\mathbb{B}) \leq \max\{g_1, g_2\},$$

where $g_1 = \Upsilon(B_{11}) + \|B_{12}\|$ and $g_2 = \|B_{21}\| + \Upsilon(B_{22})$. Clearly, $\|B_{12}\| = \|B_{21}\| = 0$ and $\Upsilon(B_{11}) = \Upsilon(B_{22}) = -(\mu + \gamma) + \frac{\dot{I}}{I_v} - \frac{\dot{I}_v}{I_v}$. Hence, we have

$$\Upsilon(\mathbb{B}) \leq -(\mu + \gamma) + \frac{\dot{I}}{I_v} - \frac{\dot{I}_v}{I_v},$$

which gives

$$\Upsilon(\mathbb{B}) \le \frac{\dot{I}}{I} - (\mu + \gamma) - \eta\frac{E_v}{I_v} + \mu.$$

Using uniform persistent result (Lemma 1) when $R_0 > 1$, we obtain

$$\Upsilon(\mathbb{B}) \le \frac{\dot{I}}{I} - (\gamma + \eta).$$

Integrating the above from 0 to t, we obtain

$$\int_0^t \Upsilon(\mathbb{B})\mathrm{d}s \le \int_0^t \frac{\dot{I}}{I}\mathrm{d}t - \int_0^t (\gamma + \eta)\mathrm{d}t,$$

i.e.,

$$\frac{1}{t}\int_0^t \Upsilon(\mathbb{B})\mathrm{d}s \le \frac{1}{t}\ln\left(\frac{I(t)}{I(0)}\right) - (\gamma + \eta).$$

Furthermore, we have

$$\limsup_{t\to\infty} \sup_{(I(0),I_v(0))\in\mathcal{K}} \frac{1}{t}\int_0^t \Upsilon(\mathbb{B})\mathrm{d}s \le -(\gamma + \eta) \le 0$$

using the boundedness of $I(t)$. We obtain $\tilde{q}_2 < 0$. Thus, the system (11) is globally asymptotically stable when $R_0 > 1$, i.e.,

$$I(t) \to I_* \quad \text{and} \quad I_v(t) \to I_{v_*} \quad \text{whenever } t \to \infty.$$

Now from the first equation of the model system (2), we have

$$\frac{\mathrm{d}S}{\mathrm{d}t} = \mu_1 N - \frac{\beta S I_v}{N_v} - \frac{\alpha S I}{N} - \mu_1 S - \theta S,$$

and the limiting form is given as follows:

$$\frac{\mathrm{d}S}{\mathrm{d}t} = \mu_1 N - \frac{\beta S I_v^*}{N_v} - \frac{\alpha S I^*}{N} - \mu_1 S - \theta S,$$

i.e.,

$$\frac{\mathrm{d}S}{\mathrm{d}t} + \left(\frac{\beta I_v^*}{N_v} + \frac{\alpha I^*}{N} + \mu_1 + \theta\right)S = \mu_1 N.$$

The above differential equation is linear in S, hence $S \to \frac{\mu_1 N}{\left(\frac{\beta I_v^*}{N_v} + \frac{\alpha I^*}{N} + \mu_1 + \theta\right)} = S^*$ whenever $t \to \infty$. Using similar argument, we can show that $E \to E^*$, $S_v \to S_v^*$, and $E_v \to E_v^*$, whenever $t \to \infty$. Hence, the endemic equilibrium point E_1 of the model system (2) is globally asymptotically stable in the sense of $(S, E, I, S_v, E_v, I_v) \to (S^*, E^*, I^*, S_v^*, E_v^*, I_v^*)$ whenever $t \to \infty$. Finally, we state the above discussion in the following result.

Theorem 8. *If $R_0 > 1$, then the unique endemic equilibrium point E_1 of the model system* (2) *is globally asymptotically stable.*

4 Bifurcation analysis at $R_0 = 1$

This part devotes to explore and determine the direction of bifurcation around $R_0 = 1$, and center manifold theory is adopted for the same as discussed in Castillo-Chavez and Song [6]. We consider the model system (2) as

$$\begin{aligned}
\frac{dx_1}{dt} &= \mu_1 N - \frac{\beta x_1 x_6}{N_v} - \frac{\alpha x_1 x_3}{N} - \mu_1 x_1 - \theta x_1 \equiv f_1,\\
\frac{dx_2}{dt} &= \frac{\beta x_1 x_6}{N_v} + \frac{\alpha x_1 x_3}{N} - \kappa x_2 - \mu_1 x_2 \equiv f_2,\\
\frac{dx_3}{dt} &= \kappa x_2 - \gamma x_3 - \mu_1 x_3 \equiv f_3,\\
\frac{dx_4}{dt} &= \mu N_v - \mu x_4 - \frac{\beta_v x_3 x_4}{N} \equiv f_4,\\
\frac{dx_5}{dt} &= \frac{\beta_v x_3 x_4}{N} - (\mu + \eta) x_5 \equiv f_5,\\
\frac{dx_6}{dt} &= \eta x_5 - \mu x_6 \equiv f_6.
\end{aligned} \tag{12}$$

The parameter β is considered as bifurcation parameter. The threshold value of bifurcation parameter is $\beta^* = \frac{(1-2R_{01})acdbNN_v}{\eta\kappa\beta_v S_0 S v_0}$ at $\beta = \beta^*$ ($R_0 = 1$). The linearized matrix at (E_0, β^*) of the model system (12) is given as follows:

$$J_{E_0}(\beta^*) = \begin{pmatrix}
-e & 0 & -\frac{\alpha S_0}{N} & 0 & 0 & -\frac{\beta^* S_0}{N_v}\\
0 & -a & \frac{\alpha S_0}{N} & 0 & 0 & \frac{\beta^* S_0}{N_v}\\
0 & \kappa & -b & 0 & 0 & 0\\
0 & 0 & -\frac{\beta_v S_{v0}}{N} & -d & 0 & 0\\
0 & 0 & \frac{\beta_v S_{v0}}{N} & 0 & -c & 0\\
0 & 0 & 0 & 0 & \eta & -d
\end{pmatrix}.$$

Clearly note that the above matrix is the same as matrix (5). Then, the corresponding characteristic polynomial are also same, and hence, the matrix $J_{E_0}(\beta^*)$ has a simple eigenvalue zero at $R_0 = 1$ along with remaining negative eigenvalues. In addition, the zero eigenvalue of $J_{x^*}(\beta^*)$, the right and left eigenvectors are given by $(w_1, w_2, w_3, w_4, w_5, w_6)^T$ and $(v_1, v_2, v_3, v_4, v_5, v_6)^T$, respectively, where $w_1 = -\frac{ab}{d\kappa}$, $w_2 = \frac{b}{\kappa}$, $w_3 = 1$, $w_4 = -\frac{\beta_v S_{v0}}{N\mu}$, $w_5 = \frac{\beta_v S_{v0}}{Nc}$, $w_6 = \frac{\beta_v S_{v0}\eta}{Nc\mu}$, and $v_1 = 0$, $v_2 = 1$, $v_3 = \frac{a}{\kappa}$, $v_4 = 0$, $v_5 = \frac{\eta\beta^* S_0}{c\mu N_v}$, and $v_6 = \frac{\beta^* S_0}{\mu N_v}$. Now, the nonzero second-order partial derivatives of f_1, f_2, f_3, f_4, f_5, and f_6 at (E_0, β^*) are given as: $\frac{\partial^2 f_1}{\partial x_1 \partial x_6} = \frac{-\beta^*}{N_v}$, $\frac{\partial^2 f_1}{\partial x_1 \partial x_3} = \frac{-\alpha}{N}$, $\frac{\partial^2 f_2}{\partial x_1 \partial x_6} = \frac{\beta^*}{N_v}$, $\frac{\partial^2 f_2}{\partial x_1 \partial x_3} = \frac{\alpha}{N}$, $\frac{\partial^2 f_5}{\partial x_3 \partial x_4} = \frac{-\beta_v}{N}$, $\frac{\partial^2 f_5}{\partial x_3 \partial x_4} = \frac{\beta_v}{N}$, $\frac{\partial^2 f_1}{\partial x_6 \partial \beta} = \frac{-x_1}{N_v}$, $\frac{\partial^2 f_2}{\partial x_6 \partial \beta} = \frac{x_1}{N_v}$.

As per our requirement, which is given in [6], we compute two important parameters $a_1 = \sum_{k,i,j=1}^{n} v_k w_i w_j \frac{\partial^2 f_k}{\partial x_i x_j}$ and $b_1 = \sum_{k,i=1}^{n} v_k w_i \frac{\partial^2 f_k}{\partial x_i \beta^*}$ as follows:

$$a_1 = -\left(\frac{2ab\beta_v S_{v0}\eta\beta^*}{d\kappa Nc\mu N_v} + \frac{2ab\alpha}{d\kappa N} + \frac{2\beta^*\beta_v^2 S_0 S_{v0}\eta}{c\mu^2 N^2 N_v}\right) \quad \text{and} \quad b_1 = \frac{\beta^* S_0 S_{v0}\eta}{N N_v c\mu}.$$

Note that a_1 is always negative, and b_1 is always positive. Thus, the forward bifurcation occurs at $R_0 = 1$, and the corresponding result is given below.

Theorem 9. *For the model system* (2)*, the direction of bifurcation is forward at* $R_0 = 1$.

Remark 2. This forward bifurcation result infers that as the basic reproduction number R_0 crosses unity, a DFE point loses its stability, and correspondingly, a stable endemic equilibrium occurs without any parametric constraints. This result supports and validates the local stability result for the endemic equilibrium point E_1 as given in Theorem 5.

5 Sensitivity analysis

In this section, our aim is to determine the key parameters of the model system, which have a significant influence on the system behavior and pattern. To accomplish this task, we initially conduct a local sensitivity analysis utilizing normal forward sensitivity indices [13]. This method determines how variations in specific parameters affect the basic reproduction number (R_0), which represents the severity of disease propagation. The normalized forward sensitivity indices concerning a particular parameter (δ) are defined as follows:

$$\gamma_{\delta}^{R_0} = \frac{\partial R_0}{\partial \delta} \times \frac{\phi}{R_0}.$$

This formula is utilized to evaluate the sensitivity of R_0 concerning a particular parameter (δ). Simply, it indicates how receptive R_0 is to changes in ϕ, taking into account the magnitude of the parameters δ and R_0. In our study, these sensitivity indices have been calculated and are presented in Figure 1 with the parametric values listed in Table 1. Parameters such as $\alpha, \beta, \beta_v, \kappa$, and η have a positive sensitivity index, signifying that an increase in these parametric values results in a corresponding increase in R_0. This suggests that alterations in these parameters could potentially heighten disease transmission. On the other hand, parameters with negative sensitivity indices, such as γ, μ_1, and μ, demonstrate that an augmentation in their values leads to a decrease in R_0, indicating that these parameters could contribute to reducing the likelihood of disease spread. Furthermore, the sensitivity index for β and β_v is identical, signifying that both β and β_v play an equal role in influencing disease transmission. Therefore, local sensitivity analysis is instrumental in identifying the factors that impact disease transmission most significantly and consequently aids decision-makers in devising public health interventions.

Global sensitivity analysis (GSA) is a potent method used to understand how changes in model parameters impact the results of a model. One effective approach for conducting GSA is by using the partial rank correlation coefficient (PRCC) in conjunction with Latin hypercube sampling (LHS) [27,32]. The magnitude

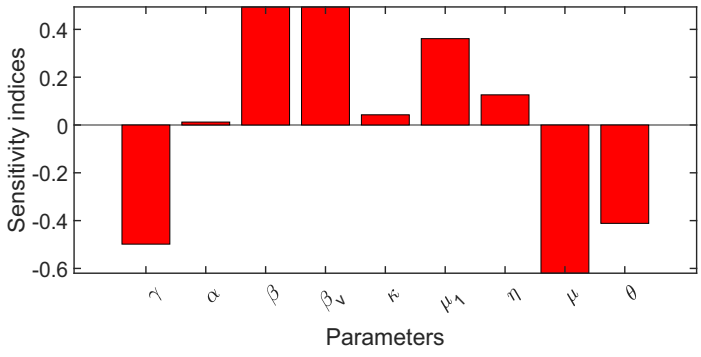

Figure 1: Normalized forward sensitivity indices of R_0.

Table 1: Parametric values used for numerical simulations

Parameters	Values	Source
β	0.75	[31]
μ_1	0.0046	[31]
θ	0.02	[32]
β_v	0.5750	Assumed
γ	0.3	[31]
μ	0.0343	[31]
κ	0.05	[31]
η	0.1	[33]
α	0.1	[9,35]

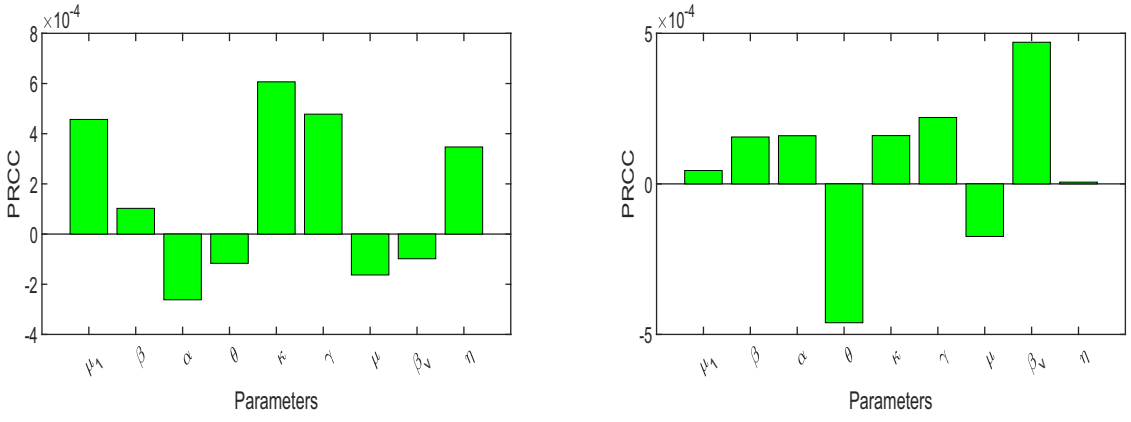

Figure 2: PRCC representation of infection classes (a) I and (b) I_v.

of the PRCC value indicates the strength of a parameter's influence on the model's behavior. A positive PRCC suggests a positive correlation, indicating that as the parameter increases, the model's output also tends to increase. In contrast, a negative PRCC indicates a negative correlation, suggesting that an increment in the parameter leads to decrease in the model's output. In this method, we executed 100 simulations for each LHS setup, beginning with baseline parameter values derived from Table 1. We introduced variations of ±25% to these parameters. The PRCC values are calculated for various parameters of system (2) over 1000 days, and their impacts on the infected human population (I) and the infected vector population (I_v) are analyzed, and the corresponding results are presented in Figure 2. A key finding of our study is the positive PRCC value linked with β in the infected population. This indicates that a rise in the value of β leads to an increase in the infected population, signifying a direct relationship. In practical terms, a higher transmission rate (β) is associated with a greater probability of individuals getting infected, which could be due to factors such as increased contact rates or enhanced infectiousness. Moreover, as illustrated in Figure 2a, the negative PRCC value associated with θ suggests that an increase in the value of θ (representing the information-induced self-protection) leads to decrease in the number of infective individuals.

6 Numerical experimentation and discussion

The aim of this section is to validate the obtained analytical results numerically and to investigate further the model's effectiveness in capturing the effect of information as individual's self-protection (θ) and direct

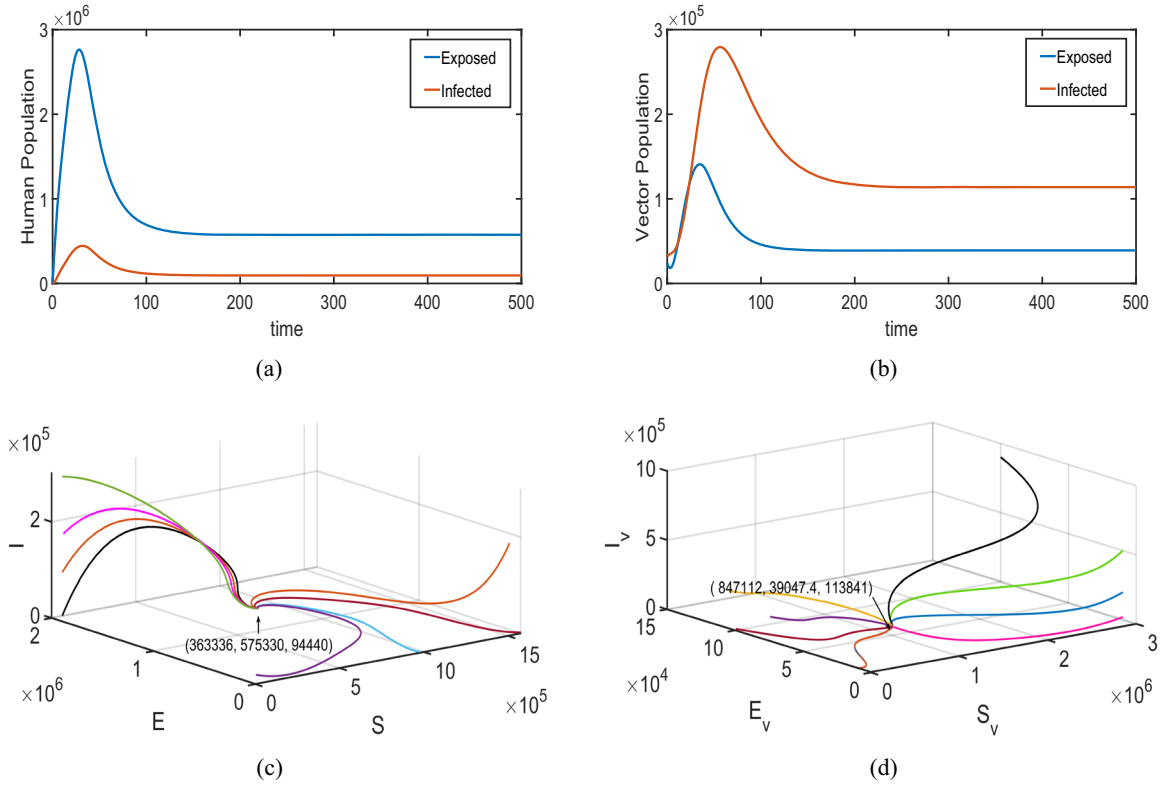

Figure 3: (a) Solution trajectories of human population approaching to endemic equilibrium point. (b) Solution trajectories of vector population approaching to endemic equilibrium point. (c) Global stability of endemic equilibrium point E_1 in SEI plane. (d) Global stability of endemic equilibrium point E_1 in $S_v E_v I_v$ plane.

transmission (α) with its biological understanding. For this purpose, we shall perform the numerical simulations and make a comparative study with help of MATLAB. The set of parameters for the simulation purpose is given in Table 1, and most of them have been chosen based on the occurrence of outbreak of South Sulawesi as reported in [31]. The initial population size is considered as: $S_0 = 8{,}768{,}197$, $E_0 = 1{,}878$, $I_0 = 1{,}895$, $S_v(0) = 944{,}000$, $E_v(0) = 24{,}000$, and $I_v(0) = 32{,}000$ along with the time period of 120 days. Thus, with the help of these parameters and numerical experimentation, we shall try to explore the biological insights of the proposed model, which may reflect the real-world dynamics of Zika transmission. This approach will allow us to quantitatively assess the effectiveness of our model in capturing the key features of the disease and the impact of information and direct transmission.

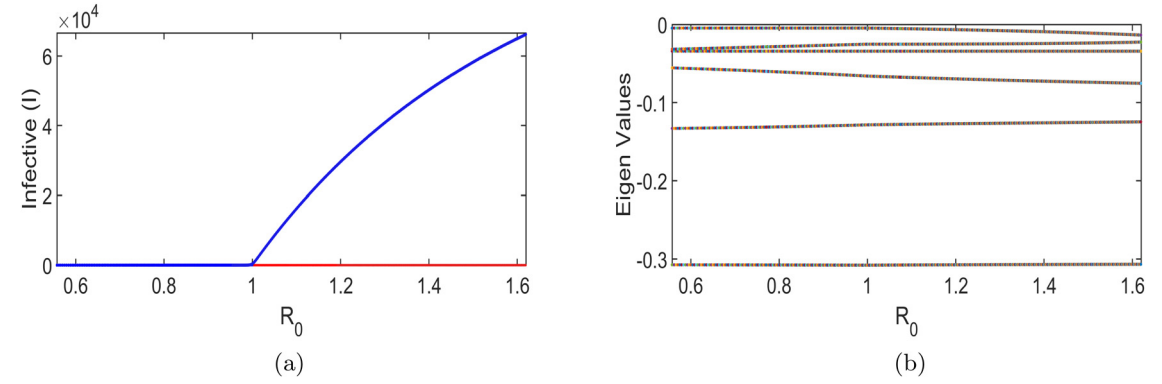

Figure 4: (a) Existence of forward bifurcation at $R_0 = 1$. (b) Real part of the eigenvalues corresponding to equilibrium points.

Example 1. In this example, we shall discuss and validate the stability properties of the equilibrium points numerically. Initially, by taking μ_1 as 4.6×10^{-5}, while retaining the other parameter values as given in Table 1, we identified that the system exclusively possesses a DFE $E_0 = (20129.23, 0, 0, 10{,}00{,}000, 0, 0)$ along with the basic reproduction number 0.267837, which is less than unity. This observation leads to validate the global stability of DFE (E_0), and Theorem 7 holds true. Furthermore, with the same parameters in Table 1, the system attains a unique endemic equilibrium point $E_1 = (363336, 575330, 94440, 847112, 39047.4, 113841)$ along with the basic reproduction number $R_0 = 2.32239$, which is greater than unity. The eigenvalues corresponding to E_1 are $\lambda_1 = -0.3138$, $\lambda_2 = -0.01330 + 0.06270i$, $\lambda_3 = -0.01330 - 0.06270i$, $\lambda_4 = -0.02610 + 0.01080i$, $\lambda_5 = -0.02610 - 0.01080i$, and $\lambda_6 = -0.0472$. Notably, the real parts of all these eigenvalues are negative, suggesting that the system is locally stable, which refers to Theorem 5. Furthermore, from Theorem 8, it clear that the endemic equilibrium point is globally stable for $R_0 > 1$. In this case, one can note that $R_0 = 2.32239 > 1$, which suffices that E_1 is globally stable. As depicted in Figure 3, the trajectories of exposed and infected populations, illustrated with blue and green curves for the human and vector populations, respectively, converge toward the endemic equilibrium point E_1 (globally stable).

Example 2. In this case, the existence of forward bifurcation for the proposed model system is validated numerically. For this purpose, the disease transmission rate β is chosen as bifurcation parameter. Furthermore, to draw the bifurcation depiction, we select the parameters given in Table 1 with $\theta = 0.0001$ and vary the parameter $\beta \in [0.0037, 0.59]$, which is equivalent to $0.562 \leq R_0 \leq 1.626$($R_0 = 1$ for $\beta = \beta^* = 0.0192$), and the corresponding result is presented in Figure 4. Clearly, one can observe that Figure 4(a) represents the forward bifurcation in which the DFE changes its stability (stable to unstable) and a unique stable endemic equilibrium (blue color curve) exists along with unstable DFE (red color curve) when R_0 crosses the unity. This observation is supported by the real part of the corresponding eigenvalues of the equilibria as presented in Figure 4(b) and all

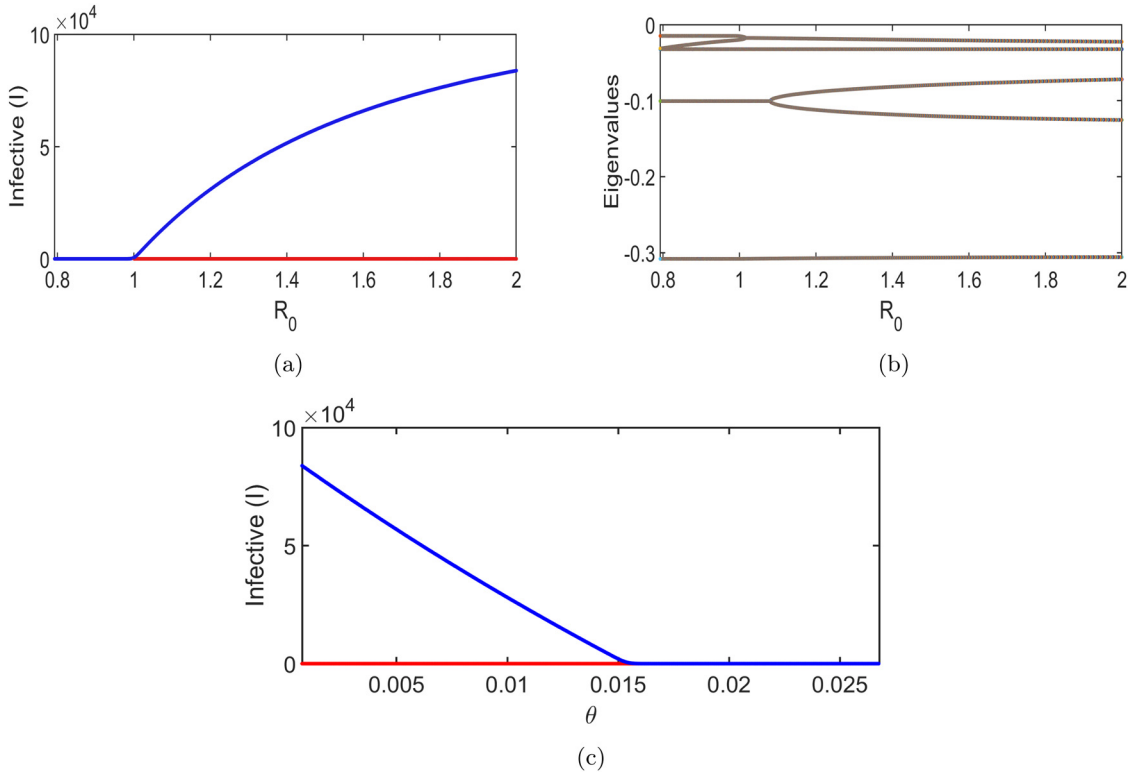

Figure 5: (a) The existence of forward bifurcation with respect to $R_0 = 1$ varying θ. (b) The corresponding plot for real parts of eigenvalues. (c) The bifurcation plot with respect to θ.

the real parts are with negative sign (stability). For particular $\beta = 0.05$, we obtain $R_0 = 1.51024 > 1$ along with $a_1 < 0$ and $b_1 < 0$. Hence, the existence of forward bifurcation is ensured (Theorem 9).

Remark 3. (Physical relevance of forward bifurcation) The above example is describing a scenario in which a disease can either die out or become endemic in a population, depending on the value of the transmission rate β. If β is low such that $R_0 < 1$, the disease cannot sustain itself, and the population remains disease-free. However, if β is greater than 0.0192, the disease can persist in the population, leading to an endemic state. Hence, the existence of the forward bifurcation infers that as the rate of Zika transmission β crosses a threshold value, the system's behavior changes between disease-free and endemic states, and hence, number of Zika cases will persist within the population.

Example 3. In this example, we validate the existence of forward bifurcation numerically corresponding to the parameter for information-induced self-protection θ (considered as bifurcation parameter). For this purpose, we consider the parametric values as given in Table 1 with $\beta = 0.1$ and $\theta \in [0.000743592, 0.0267891]$, which is equivalent to $2 \geq R_0 \geq 0.7923$ (as θ and R_0 have reverse nature) and the corresponding value of $\theta = \theta^* = 0.0153914$ $(R_0 = 1)$. The corresponding bifurcation results of forward bifurcation is shown in Figure 5. Clearly, one can observe from Figure 5(a) that as R_0 crosses unity, the DFE (red color curve) loses its stability, whereas the endemic equilibrium (blue color curve) becomes stable. This signifies the coexistence of unstable DFE with stable endemic equilibrium for $R_0 > 1$. The real parts of the eigenvalues corresponding to the equilibrium point is shown in Figure 5(b). In order to see the effect of θ, we also plotted the bifurcation curve in Figure 5(c) and one can observe a similar kind of pattern. Hence, the existence of forward bifurcation is ensured using information-induced self-protection (θ) as bifurcation parameter.

Example 4. In this case, we shall explore the effect of various model parameters on the basic reproduction number as it determines the persistence of the Zika within the population. From the basic reproduction number (R_0) of the model, we observe that $\frac{\partial R_0}{\partial \theta} < 0$, which infers that as information-induced self-protection (θ) increases, the corresponding R_0 decreases, which implies that higher self-protection leads to keep a tab on the disease prevalence. Similarly, $\frac{\partial R_0}{\partial \alpha} > 0$ (as α increases, R_0 increases, and *vice versa*), thus one can observe that as vertical transmission (less sexual contact and others less direct mode) is minimal, the Zika prevalence will also be minimal. A similar kind of argument also works for the case of disease transmission (β) as $\frac{\partial R_0}{\partial \beta} > 0$. Further to observe these facts, we generated surface plots of R_0 with respect to model parameters θ, α and β whereas the other parameters are same as in Table 1 and the corresponding results are presented in Figure 5. A similar kind of observations are also obtained and matched with results as discussed in sensitivity analysis section (forward indices and PRCC).

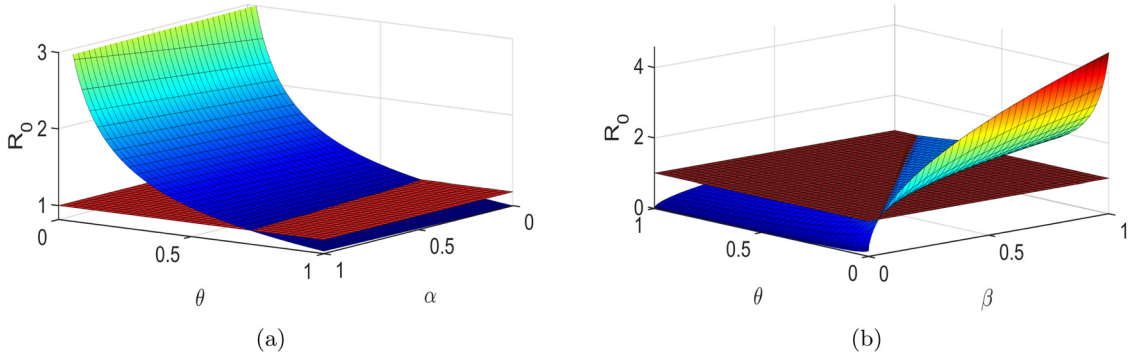

Figure 6: R_0 with respect to (a) α and θ. (b) β and θ.

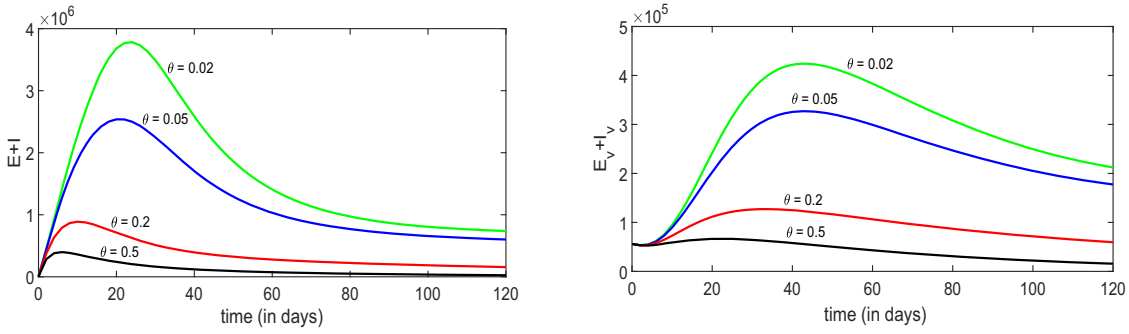

Figure 7: Effect of self-protection (θ) on the population (a) $E + I$ and (b) $E_v + I_v$.

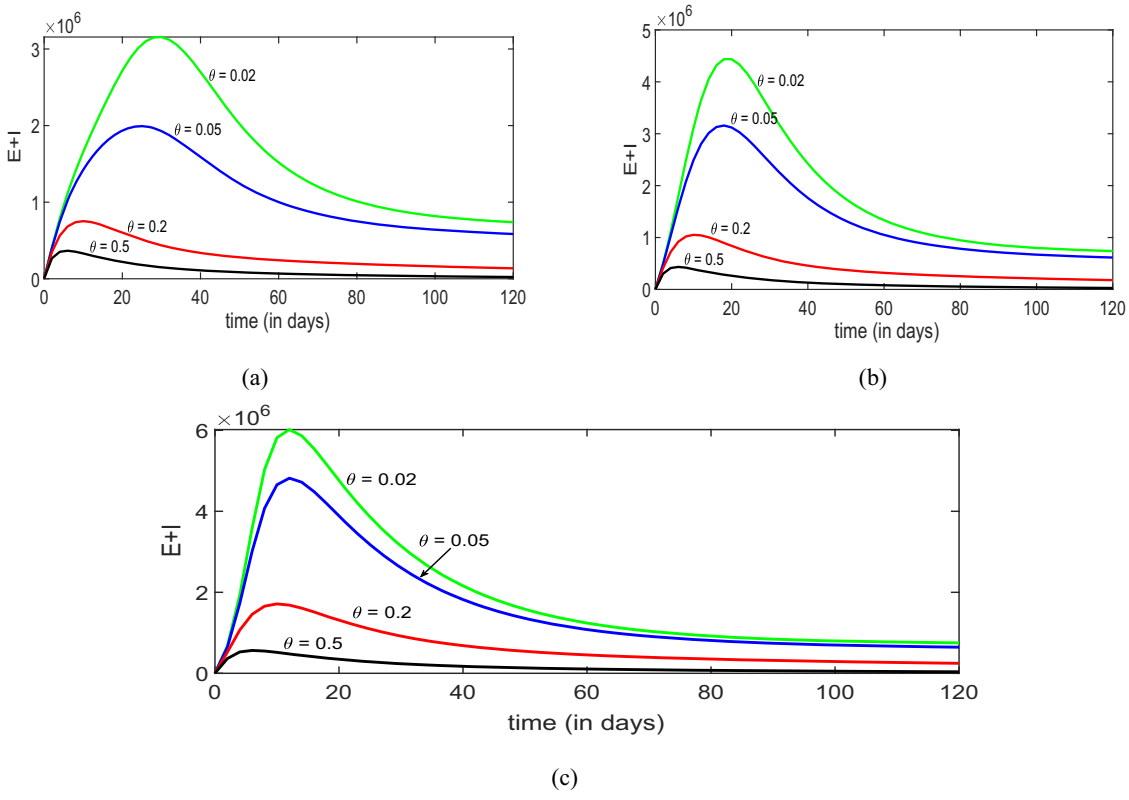

Figure 8: Impact of self-protection on cumulative count of infection ($E + I$) for (a) $\alpha = 0$, (b) $\alpha = 0.2$, and (c) $\alpha = 0.5$.

6.1 Impact of important parameters on the Zika prevalence

This particular segment is devoted to explore the effect of various model parameters on the Zika transmission by performing a comparative study numerically.

6.1.1 Effect of self-protection (θ) and direct transmission (α)

In the proposed model, we have quantified the effect of important parameters, such as θ and α, which represent the impact of information-based self-protection and the direct transmission rate, respectively.

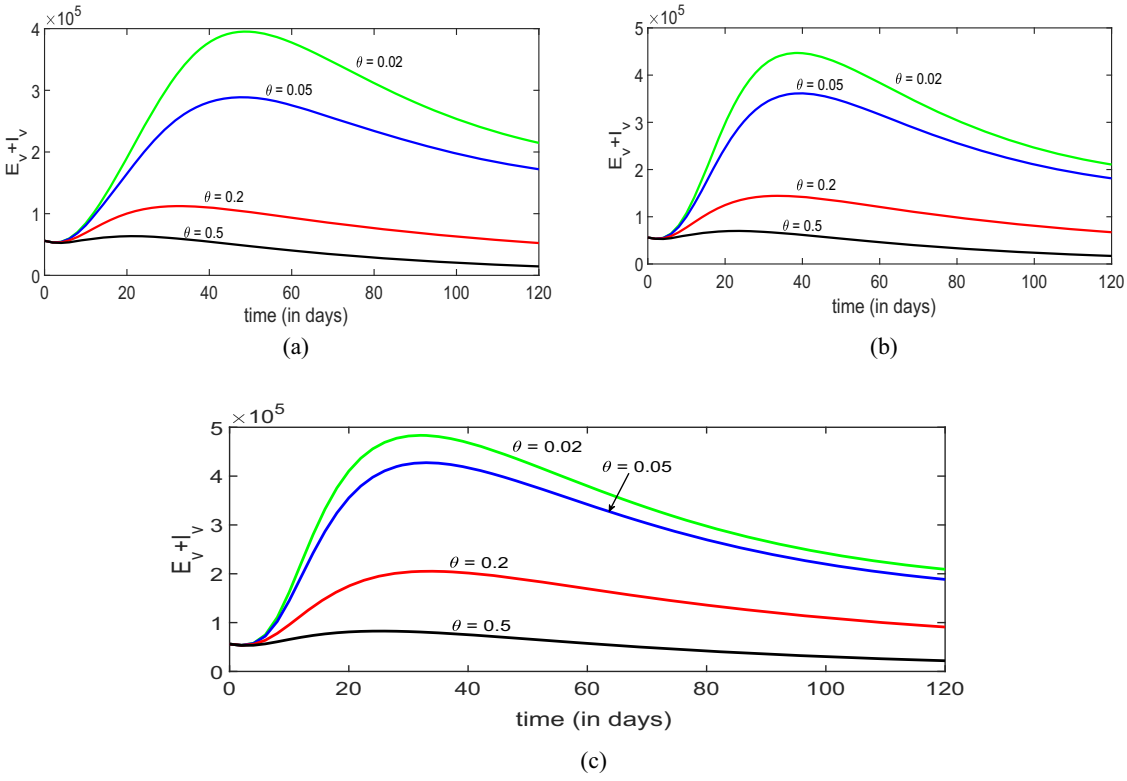

Figure 9: Impact of self-protection on cumulative count of vector population ($E_v + I_v$) for (a) $\alpha = 0$ (b) $\alpha = 0.2$, and (c) $\alpha = 0.5$.

However, exploring their impact on Zika prevalence analytically is challenging due to complex nature of model. Therefore, to understand the influence of information-based self-protection (θ) and the direct transmission rate (α), we shall conduct a comparative study numerically. This will involve analyzing the cumulative count of infections, which includes both exposed and infected individuals, under various values of these parameters. The obtained comparative results of this study are presented in Figures 7–9. Initially, as depicted in Figure 7, we have plotted the population trajectories of the model for different values of θ along with other parameters as given in Table 1. We observed that as the self-protection due to information (θ) increases, there is a noticeable reduction in the peak and prevalence of the cumulative Zika cases within the population. This is evident from the comparison between the black color curve (high self-protection and lower disease prevalence) and the green color curve (less self-protection and higher disease prevalence). This observation

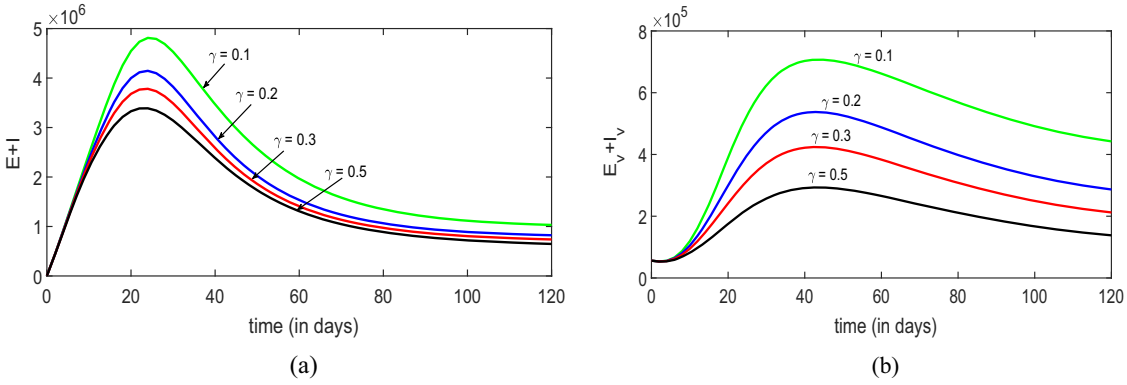

Figure 10: Effect of recovery (γ) on infection classes for (a) $E + I$ and (b) $E_v + I_v$.

highlights the tangible benefits of self-protection measure in controlling the spread of the Zika within the community.

Subsequently, we explore the impact of information-induced self-protection on the infected population for different degrees of direct transmission (α), and the outcomes are presented in Figures 8 and 9. It is noted that a rise in direct transmission leads to an increase in the cumulative count of infections. However, the effect of self-protection remains highly effective in moderating the cumulative count of infections in both human and vector populations. Clearly, a comparison can be made easily between Figure 8(b) and (c) (black and green colored curves). In both cases, even if the direct transmission rate increases (0.2 to 0.5), the effect of self-protection (lower to higher) also plays a crucial role and significantly suppresses the infection (black colored curves). This observation emphasizes the importance of disseminating information, which influences the individuals behavioral response to encourage self-protective behavior to adopt suitable measures to combat the Zika infection. Hence, the comparison among the outcomes presented in Figures 7–9 illustrates the balance between direct transmission rate and self-protection in determining the disease dynamics within the community.

6.1.2 Effect of recovery rate (γ)

Once a healthy individual becomes infected, recovery through treatment or natural means plays an important role in treating the infected person so that disease burden can be minimized. Therefore, we shall assess the effect of the recovery rate (γ) on Zika prevalence by changing the degree of its numerical values of γ keeping other parametric values fixed as given in Table 1. The numerical outcomes of this comparison are displayed in Figure 10. Our investigation indicates that as the recovery rate (γ) increases, there is a discernible reduction in the cumulative number of infected cases in both the host and vector populations, transitioning from the green to black curves in Figure 10(a) and (b). This implies that enhancing the recovery rate is crucial in controlling the disease, and effective measures must be implemented by policymakers to achieve predefined objectives related with disease and economic burdens. In conclusion, our analysis reveals that the combined effects of heightened self-protection and recovery play a substantial role in reducing the overall count of infections across both human and vector populations.

7 Conclusion

In this study, we formulated and analyzed a nonlinear SEI-type compartmental mathematical model for Zika transmission incorporating vertical transmission mechanisms such as direct sexual contact and mother-to-fetus transmission. As per WHO suggestions, individual self-protection plays a key role in combating the infection [40], and at the same time, information about a disease prevalence also alters the nature of individuals. Therefore, keeping these facts in mind to control the Zika transmission, we quantified the effect of information-induced self-protection as a control measure on the healthy population to adopt suitable precautionary measures. We determined the basic reproduction numbers (R_0), which provide insights into the disease's persistence and potential spread within the population. The model analysis is performed, and local stability properties of equilibrium points are also established. In addition, the global stability for both disease-free and endemic equilibrium is also determined using a geometric approach. Furthermore, the central manifold theory is employed to determine the existence of forward bifurcation around R_0 equal to one and claimed the existence of forward bifurcation. Local and global sensitivity analyses are conducted to examine the impact of various parameters using normalized forward sensitivity index and PRCC methods, respectively. Our study also explored the effects of self-protection (θ), direct transmission rate (α), and recovery rate (γ) on both human and vector populations. It is found that an increment in self-protection leads to a decrease in the infected count highlighting the critical role of information-based self-protection in reducing infection numbers even if direct transmission is very high. Moreover, a higher recovery rate is identified as a key factor in

minimizing the peak of Zika cases within the population. Moreover, there is an indirect relation between the information-based self-protection and recovery rate due to the awareness about the protective measures and health care measures. When individuals are well-informed about the disease and their consequences, they are more likely to adopt preventive measures, such as practicing good hygiene, using mosquito repellent, bed nets, full-sleeve cloths, adhering to safety guidelines, and many more. In addition, informed individuals are more active in seeking appropriate medical care timely. This informed behavior contributes to a reduction in the overall number of infections within the population. With fewer individuals falling ill, medical resources can be allocated more efficiently, and treatments can be administered more effectively for a large proportion of the population, which enhance the recovery rate. Thus, these two factors recover via medical treatment and information-based self-protection (both are indirectly connected) play a crucial role. In conclusion, this study emphasizes the importance of information-based self-protection on Zika transmission, which significantly reduces the peak and duration of Zika cases, whereas a higher recovery rate also controls the spread of Zika virus and reduces the disease burden.

Acknowledgement: The authors are grateful to the anonymous reviewers for their constructive comments, which helped in strengthen the manuscript.

Funding information: This research received no specific grant from any funding agency, commercial or nonprofit sectors.

Conflict of interest: The authors have no conflicts of interest to disclose.

Ethical approval: This research did not require ethical approval.

References

[1] Abidemi, A., Ackora-Prah, J., Fatoyinbo, H. O., & Asamoah, J. K. K. (2022). Lyapunov stability analysis and optimization measures for a dengue disease transmission model. *Physica A: Statistical Mechanics and its Applications*, *602*, 127646.

[2] Al-Maqrashi, K., Al-Musalhi, F., Elmojtaba, I., & Al-Salti, N. (2023). Mathematical analysis and parameter estimation of a two-patch Zika model. *Letters in Biomathematics*, *10*(1), 29–41.

[3] Biswas, S. K., Ghosh, U., & Sarkar, S. (2020). Mathematical model of Zika virus dynamics with vector control and sensitivity analysis. *Infectious Disease Modelling*, *5*, 23–41.

[4] Brauer, F., Castillo-Chavez, C., Mubayi, A., & Towers, S. (2016). Some models for epidemics of vector-transmitted diseases. *Infectious Disease Modelling*, *1*(1), 79–87.

[5] Castillo-Chavez, C., Feng, Z., & Huang, W. (2002). On the computation of RO and its role in global stability. *Institute for Mathematics and Its Applications*, *125*, 229.

[6] Castillo-Chavez, C., & Song, B. (2004). Dynamical models of tuberculosis and their applications. *Mathematical Biosciences and Engineering*, *1*(2), 361–404.

[7] Coppel, W. (1965). Stability and asymptotic behavior of differential equations. *Heath*, *80*, 17–30.

[8] De Lara-Tuprio, E. P., Teng, T. R. Y., & Macalalag, J. M. R. (2021). Global stability analysis of dengue transmission model with awareness, vector control and time delays. In: *Journal of Physics: Conference Series* (Vol. 1899, p. 012104). Makassar, Indonesia: IOP Publishing.

[9] Denu, D., & Son, H. (2022). Analysis and optimal control of a deterministic Zika virus model. *Journal of Nonlinear Sciences & Applications (JNSA)*, *15*(2), 88–108.

[10] Fact-sheet of Vector-borne diseases. 2020. https://www.who.int/news-room/fact-sheets/detail/vector-borne-diseases.

[11] Freedman, H., Ruan, S., & Tang, M. (1994). Uniform persistence and flows near a closed positively invariant set. *Journal of Dynamics and Differential Equations*, *6*(4), 583–600.

[12] Gao, D., Lou, Y., He, D., Porco, T. C., Kuang, Y., Chowell, G., & Ruan, S. (2016). Prevention and control of zika as a mosquito-borne and sexually transmitted disease: a mathematical modeling analysis. *Scientific Reports*, *6*(1), 1–10.

[13] Ghosh, I., Tiwari, P. K., & Chattopadhyay, J. (2019). Effect of active case finding on dengue control: Implications from a mathematical model. *Journal of Theoretical Biology*, *464*, 50–62.

[14] Gubler, D. J. (1998). Dengue and dengue hemorrhagic fever. *Clinical Microbiology Reviews*, *11*(3), 480–496.

[15] Hasan, B. (2018). *A study on numerical modeling of vector-borne diseases*. (PhD thesis). Australia: Swinburne University of Technology.
[16] Ibrahim, M., & Dénes, A. (2023). A mathematical model for zika virus infection and microcephaly risk considering sexual and vertical transmission. *Axioms*, *12*, 263.
[17] Kassa, S. M., & Ouhinou, A. (2011). Epidemiological models with prevalence dependent endogenous self-protection measure. *Mathematical Biosciences*, *229*(1), 41–49.
[18] Kassa, S. M., & Ouhinou, A. (2015). The impact of self-protective measures in the optimal interventions for controlling infectious diseases of human population. *Journal of Mathematical Biology*, *70*, 213–236.
[19] Kumar, A., & Srivastava, P. K. (2023). Role of optimal screening and treatment on infectious diseases dynamics in presence of self-protection of susceptible. *Differential Equations and Dynamical Systems*, *31*(1), 135–163.
[20] Kumar, A., Srivastava, P. K., & Takeuchi, Y. (2017). Modeling the role of information and limited optimal treatment on disease prevalence. *Journal of Theoretical Biology*, *414*, 103–119.
[21] Kumar, S., Sharma, S., Kashyap, A., Kumari, N., & Agarwal, R. P. (2023). Modelling the effect of environmental pollution on Zika outbreak: A case study of Brazil. *Discrete and Continuous Dynamical Systems-S*, 2023, 1–27.
[22] Li, M., Graef, J., Wang, L., & Karsai, J. (1999). Global dynamics of a SEIR model with varying total population size. *Mathematical Biosciences*, *160*(2), 191–213.
[23] Li, M., & Wang, L. (1998). A criterion for stability of matrices. *Journal of Mathematical Analysis and Applications*, *225*(1), 249–264.
[24] Li, M. Y., & Muldowney, J. S. (1996). A geometric approach to global-stability problems. *SIAM Journal on Mathematical Analysis*, *27*(4), 1070–1083.
[25] Macalalag, J. M. R., Teng, T. R. Y., & de Lara-Tuprio, E. P. (2022). Global stability analysis of dengue model with awareness, vector control and time delays. *Towards Intelligent Systems Modeling and Simulation: With Applications to Energy, Epidemiology and Risk Assessment*, *383*, 177–195.
[26] Manfredi, P., & D'Onofrio, A. (2013). *Modeling the interplay between human behavior and the spread of infectious diseases*. New York: Springer Science & Business Media.
[27] Marino, S., Hogue, I. B., Ray, C. J., & Kirschner, D. E. (2008). A methodology for performing global uncertainty and sensitivity analysis in systems biology. *Journal of Theoretical Biology*, *254*(1), 178–196.
[28] Muldowney, J. (1990). Compound matrices and ordinary differential equations. *Rocky Mountain Journal of Mathematics*, *20*(4), 857–872.
[29] Ndaïrou, F., Area, I., Nieto, J. J., Silva, C. J., & Torres, D. F. (2018). Mathematical modeling of Zika disease in pregnant women and newborns with microcephaly in Brazil. *Mathematical Methods in the Applied Sciences*, *41*(18), 8929–8941.
[30] Park, A. W., Cleveland, C. A., Dallas, T. A., & Corn, J. L. (2019). Vector species richness increases haemorrhagic disease prevalence through functional diversity modulating the duration of seasonal transmission-erratum. *Parasitology*, *146*(10), 1353–1353.
[31] Sanusi, W., Badwi, N., Zaki, A., Sidjara, S., Sari, N., Pratama, M. I., & Side, S. (2021). Analysis and simulation of SIRS model for dengue fever transmission in south Sulawesi, Indonesia. *Journal of Applied Mathematics*, *2021*, 1–8.
[32] Srivastav, A. K., Kumar, A., Srivastava, P. K., & Ghosh, M. (2021). Modeling and optimal control of dengue disease with screening and information. *The European Physical Journal Plus*, *136*(11), 1187.
[33] Towers, S., Brauer, F., Castillo-Chavez, C., Falconar, A. K., Mubayi, A., Romero-Vivas, C. M. (2016). Estimate of the reproduction number of the 2015 Zika virus outbreak in Barranquilla, Colombia, and estimation of the relative role of sexual transmission. *Epidemics*, *17*, 50–55.
[34] Van den Driessche, P., & Watmough, J. (2002). Reproduction numbers and sub-threshold endemic equilibria for compartmental models of disease transmission. *Mathematical Biosciences*, *180*(1–2), 29–48.
[35] Wang, L., Zhao, H., Oliva, S. M., & Zhu, H. (2017). Modeling the transmission and control of Zika in Brazil. *Scientific Reports*, *7*(1), 1–14.
[36] Wang, X., Chen, Y., Martcheva, M., & Rong, L. (2020). Asymptotic analysis of a vector-borne disease model with the age of infection. *Journal of Biological Dynamics*, *14*(1), 332–367.
[37] Wei, H.-M., Li, X.-Z., & Martcheva, M. (2008). An epidemic model of a vector-borne disease with direct transmission and time delay. *Journal of Mathematical Analysis and Applications*, *342*(2), 895–908.
[38] World Health Organization, Fact sheets about Vector-borne diseases. February 2016. https://www.who.int/en/news-room/fact-sheets/detail/vector-borne-diseases.
[39] Zika epidemiology update – February 2022. https://www.who.int/publications/m/item/zika-epidemiology-update–february-2022.
[40] Zika virus. 2022. https://www.who.int/news-room/fact-sheets/detail/zika-virus.

Appendix

A Geometric approach

Here, we briefly discuss the geometric approach developed by Li and Muldowney to show the global stability of unique endemic equilibrium point E_1 [24]. Now, consider the following system:

$$\dot{x} = f(x), \tag{A1}$$

where $f : \mathcal{D} \to \mathbb{R}^n$, $\mathcal{D} \subset \mathbb{R}^n$ be an open set and the solution $x(t, x_0)$ of the system (A1) is uniquely determined by its initial value $x(0) = x_0$. Now, we further assume that:
(N1) $\mathcal{D}$ is simply connected,
(N2) x_* is the only equilibrium point of the system A1 in $\mathcal{D}$, and
(N3) there is a compact absorbing set $\mathcal{K} \subset \mathcal{D}$.

The Lozinskiĭ measure [7] of a square matrix $\mathbb{B}$ with respect to induced matrix norm $\|.\|$ is defined as follows:

$$\Upsilon(\mathbb{B}) = \lim_{h \to 0} \frac{\|I + h\mathbb{B}\| - 1}{h}.$$

Here, I is identity matrix.

Now, consider a map $x \mapsto Q(x)$, $x \in \mathcal{D}$, where $Q(x)$ is an $\binom{n}{2} \times \binom{n}{2}$-matrix-valued C^1 function, and also $Q^{-1}(x)$ exists. Now we define $\mathbb{B} = Q_f Q^{-1} + QJ^{[2]}Q^{-1}$, where the matrix Q_f is $(Q_{i,j}(f))_f$ and is obtained by $(Q_{i,j}(f))_f = \nabla Q_{i,j} \cdot f(x)$. $J^{[2]}$ is the second additive compound matrix of the Jacobian matrix J of the system (A1) [23,28]. Now, define the following quantity for the defined Lozinskiĭ measure as

$$\tilde{q}_2 = \limsup_{t \to \infty} \sup_{x_0 \in \mathcal{K}} \frac{1}{t} \int_0^t \Upsilon(\mathbb{B}(x(t, x_0)))\mathrm{d}s. \tag{A2}$$

The result of Li and Muldowney is given as follows [24].

Theorem 10. *If assumptions N_1, N_2, and N_3 hold for the system* (A1), *then the unique equilibrium x_* is globally asymptotically stable if there exist a function $Q(x)$ and Lozinskiĭ measure Υ such that $\tilde{q}_2 < 0$.*